

*XVII IMEKO World Congress
Metrology in the 3rd Millennium
June 22–27, 2003, Dubrovnik, Croatia*

INTERPOLATION IN THE FREQUENCY DOMAIN TO IMPROVE PHASE MEASUREMENT

Dušan Agrež

Faculty of Electrical Engineering, University of Ljubljana, Ljubljana, Slovenia

Abstract – Possibilities of an error reduction of the phase estimation with an interpolated discrete Fourier transform (DFT) for the rectangular window are described. Properties of interpolations are studied with respect to their ability for correction systematic effects of the used window. The correction is improved with considering the leakage effect of the component spectrum. Uncertainties of the phase estimations have been studied. The simulation and experimental results are presented showing the effectiveness in estimating the phase of the signal component.

Keywords: phase estimation, leakage effect, interpolated DFT.

1. INTRODUCTION

To estimate parameters of the time depended signals, containing any periodicity, it is most suitable to use the frequency domain. The basic parameters of periodicity are: frequency of the energy kernel f_m , amplitude of the frequency main lobe A_m and phase φ_m , i.e. the time position of the signal structure [1]. The sampled analog multi-frequency signal $g(t)$ can be written as follows:

$$g(k \Delta t)_N = \sum_{m=0}^M A_m \sin(2\pi f_m k \Delta t + \varphi_m) \quad (1)$$

Tones of the sampled signal do not always coincide with the basic set of periodic components of the discrete Fourier transformation. The position of the measurement component δ_m between DFT coefficients $G(i_m)$ and $G(i_m + 1)$ surrounding the component can be estimated by means of the interpolation [2-4]. In this paper we try to show a two-point interpolation of the DFT also for improving the phase estimation.

2. ANALYSIS OF THE DFT COEFFICIENTS

Using N samples of the signal (1), the DFT at the spectral line i is given by:

$$G(i) = -\frac{j}{2} \sum_{m=0}^M A_m [W(i - \theta_m) e^{j\varphi_m} - W(i + \theta_m) e^{-j\varphi_m}] \quad (2)$$

where θ_m is the signal frequency divided by the frequency resolution of the time window $\Delta f = 1/(N\Delta t)$ and can be written in two parts:

$$\theta_m = \frac{f_m}{\Delta f} = i_m + \delta_m \quad -0.5 < \delta_m \leq 0.5 \quad (3)$$

where i_m is an integer value and the displacement term δ_m is caused by the non-coherent sampling.

The DFT coefficients surrounding one component in the signal are due to the short-range leakage contribution of the window spectrum weighted by the amplitude of the frequency component (from the first term in (2)) and the long-range leakage contributions. For one component only, the expression (2) can be reduced:

$$G(i) = -j \frac{A_m}{2} [W(i - \theta_m) e^{j\varphi_m} - W(i + \theta_m) e^{-j\varphi_m}] \quad (4)$$

If the function $W(\theta)$ of window used is analytically known, the parameters of the signal can be estimated. For the rectangle window, the following equation is valid, where the Dirichlet kernel is used [5]:

$$W_{\text{rect.}}(\theta) = \frac{\sin(\pi\theta)}{N \sin(\pi\theta/N)} \cdot e^{-j\pi \left(\frac{N-1}{N}\right)\theta} \quad (5)$$

The largest DFT coefficient, which is mostly composed of the short-range leakage contribution of the investigated component m , can be deduced from (4) and (5) using $a = \pi(N-1)/N$ and $-j = e^{-j\pi/2}$:

$$G(i_m) = \frac{A_m}{2} \left[\frac{\sin(\pi(i_m - \theta_m))}{N \sin(\pi(i_m - \theta_m)/N)} e^{j \left[a(\theta_m - i_m) + \varphi_m - \frac{\pi}{2} \right]} - \frac{\sin(\pi(i_m + \theta_m))}{N \sin(\pi(i_m + \theta_m)/N)} e^{-j \left[a(\theta_m + i_m) + \varphi_m + \frac{\pi}{2} \right]} \right] \quad (6)$$

The component phase φ_m is referred to the start point of the window (not to the middle point [6]). Since N is usually large $N \gg 1$ and considering (3), (6) can be rewritten:

$$G(i_m) = \frac{A_m}{2} \left[\frac{\sin(\pi(-\delta_m))}{\pi(-\delta_m)} e^{j \left[a(\delta_m) + \varphi_m - \frac{\pi}{2} \right]} - \frac{\sin(\pi(2i_m + \delta_m))}{\pi(2i_m + \delta_m)} e^{-j \left[a(2i_m + \delta_m) + \varphi_m + \frac{\pi}{2} \right]} \right] \quad (7)$$

Both, amplitude and phase have additional disturbing components from the second part in (7):

$$G(i_m) = |G(i_m)| e^{j \left[a(\delta_m) + \varphi_m - \frac{\pi}{2} \right] \pm \Delta(i_m)}; \arg[G(i_m)] = \varphi_m + a\delta_m - \frac{\pi}{2} \pm \Delta\varphi(i_m) \quad (8)$$

If the displacement term is positive $0,5 > \delta_m \geq 0$, than the second largest DFT coefficient is $G(i_m + 1)$ and if the displacement term is negative $0 > \delta_m \geq -0,5$, than the second largest DFT coefficient is $G(i_m - 1)$ (Fig.1). The difference of the coefficients surrounding the largest one $G(i_m)$ gives us the sign of displacement $s = \text{sign}(|G(i_m + 1)| - |G(i_m - 1)|)$. The largest side coefficient can be expressed in common as:

$$G(i_m + s) = \frac{A_m}{2} \left[\frac{\sin(\pi(s - \delta_m))}{\pi(s - \delta_m)} e^{j[a(\delta_m - s) + \varphi_m - \frac{\pi}{2}]} - \frac{\sin(\pi(2i_m + s + \delta_m))}{\pi(2i_m + s + \delta_m)} e^{-j[a(2i_m + s + \delta_m) + \varphi_m + \frac{\pi}{2}]} \right] \quad (9)$$

$$G(i_m + s) = |G(i_m + s)| e^{j[a(\delta_m - s) + \varphi_m - \frac{\pi}{2}]} \mp \Delta(i_m + s) \quad (9a)$$

$$\arg[G(i_m + s)] = \varphi_m + a(\delta_m - s) - \frac{\pi}{2} \mp \Delta\varphi(i_m + s) \quad (9b)$$

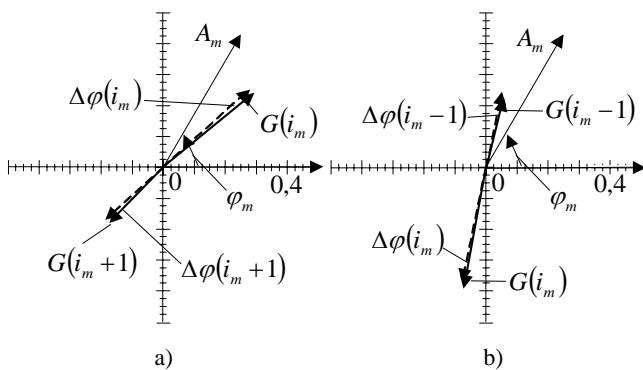


Fig. 1. Phasors diagrams for a single component $A_m = 1$ $\varphi_m = \pi/3$ and the rectangular window: a) $\theta_m = 4,4$; b) $\theta_m = 3,6$

3. PHASE ESTIMATION

In the first approximation, the second term in (7) and (9) can be neglected and the phase of component can be estimated by:

$$\varphi_m' = \arg[G(i_m)] - \pi \frac{N-1}{N} \delta_m + \frac{\pi}{2} \quad (10)$$

$$\varphi_m'' = \arg[G(i_m + s)] + \pi \frac{N-1}{N} (s - \delta_m) + \frac{\pi}{2} \quad (11)$$

We can improve the estimation by considering the long-range contributions, which have following properties:

$$\frac{\Delta\varphi(i_m)}{\Delta\varphi(i_m + s)} \cong \frac{\sin[\Delta\varphi(i_m)]}{\sin[\Delta\varphi(i_m + s)]} = \frac{|\Delta(i_m)| |G(i_m + s)|}{|G(i_m)| |\Delta(i_m + s)|} \quad (12)$$

$$\frac{|\Delta(i_m)|}{|\Delta(i_m + s)|} \cdot \frac{|G(i_m + s)|}{|G(i_m)|} = \frac{2i_m + s + \delta_m}{2i_m + \delta_m} \cdot \frac{|G(i_m + s)|}{|G(i_m)|} \quad (13)$$

If $i_m \gg 1$ is large enough, we can equalize $|\Delta(i_m)| \approx |\Delta(i_m + s)|$ and (12) can be written as:

$$\frac{\Delta\varphi(i_m)}{\Delta\varphi(i_m + s)} \cong \frac{|G(i_m + s)|}{|G(i_m)|} = \frac{\delta_m}{s - \delta_m}; \quad (s - \delta_m)\Delta\varphi(i_m) \cong \delta_m\Delta\varphi(i_m + s) \quad (14)$$

The multiplication of (10) and (11) by the correction (14) gives us estimation of the phase as an averaging of the two arguments $\arg[G(i_m)]$ and $\arg[G(i_m + s)]$ surrounding the component:

$$\bar{\varphi}_m = (1 - |\delta_m|)\arg[G(i_m)] + |\delta_m|\arg[G(i_m + s)] + \frac{\pi}{2} \quad (15)$$

Better estimation can be attained by considering also the long-range contributions (Fig. 3c):

$$\frac{\Delta\varphi(i_m)}{\Delta\varphi(i_m + s)} \cong \frac{2i_m + s + \delta_m}{2i_m + \delta_m} \cdot \frac{|G(i_m + s)|}{|G(i_m)|} = b \cdot \frac{|G(i_m + s)|}{|G(i_m)|} \quad (16)$$

$$\bar{\varphi}_m = \frac{|G(i_m)|\arg[G(i_m)] + b|G(i_m + s)|\arg[G(i_m + s)]}{|G(i_m)| + b|G(i_m + s)|} + sa \left(\frac{b|G(i_m + s)|}{|G(i_m)| + b|G(i_m + s)|} - |\delta_m| \right) + \frac{\pi}{2} \quad (17)$$

The systematic errors of the phase estimations $E = \varphi_m - \varphi_0$ (φ_0 - is the true value of the phase) are phase dependent (Fig. 2: The error curves are very close to sine like function). In simulations, the absolute maximum values of the errors at a given relative frequency were searched when phase were changed in interval $-\pi/2 \leq \varphi \leq \pi/2$ (Fig. 3). The estimation errors drop with the increasing relative frequency.

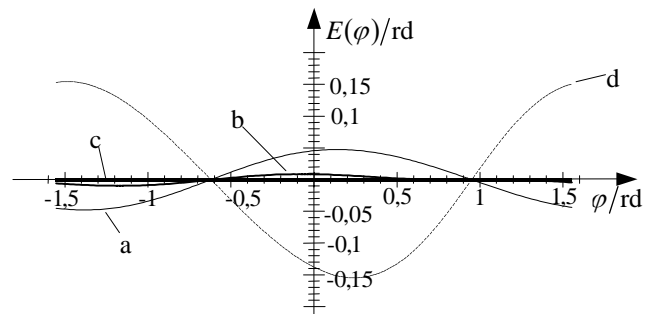


Fig. 2. Phase dependency errors at $\theta = 2,2$, $-\pi/2 \leq \varphi \leq \pi/2$; Estimations: a – by (10), b – by (15), c – by (17), d – by (11)

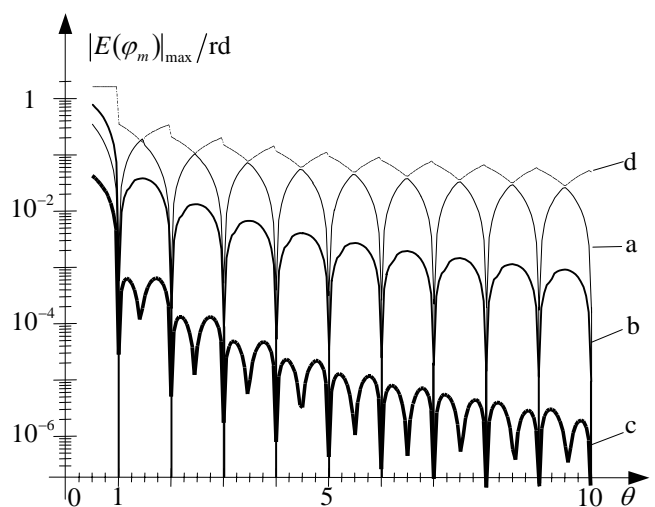


Fig. 3. Maximal systematic errors of the phase estimations: a – by (10), b – by (15), c – by (17), d – by (11); θ is known

Fig. 4 shows the importance of the frequency estimation accuracy. If the frequency is estimated by a known two-point estimation (18) [2] the overall errors increase (Fig. 4: $E_{c^*}/E_c \approx 200$).

$$\theta = i + \delta_m = i + s \frac{|G(i_m + s)|}{|G(i_m)| + |G(i_m + s)|} \quad (18)$$

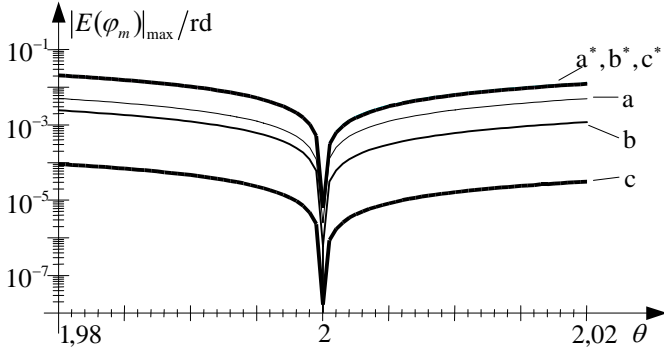


Fig. 4. Maximal systematic errors of the phase estimations in the interval $1,98 \leq \theta \leq 2,02$: a – by (10), b – by (15), c – by (17);

a^*, b^*, c^* - θ is estimated by (18)

4. UNCERTAINTY

The uncertainty propagation through the DFT procedure is well known $\sigma_R = \sigma_I = \sigma_{|G(i)|} = \sigma_{\text{DFT}} = \sigma_i / (N\sqrt{2}) \sqrt{\sum_{k=0}^{N-1} w^2(k)}$ [7], where we use $R(i) = \text{Re}[G(i)]$ and $I(i) = \text{Im}[G(i)]$ for the real and imaginary parts of the DFT and $|G(i)| = \sqrt{R^2(i) + I^2(i)}$ for the amplitude and $\varphi(i) = \arg[G(i)] = \tan^{-1}(I(i)/R(i))$ for the phase. The phase uncertainty is equal to the uncertainty of the DFT procedure scaled by the amplitude coefficient $\sigma_{\varphi(i)} = \sigma_{\text{DFT}}/|G(i)|$:

$$c_R(i) = \frac{\partial \varphi(i)}{\partial R(i)} = -\frac{I(i)}{|G(i)|^2} \quad c_I(i) = \frac{\partial \varphi(i)}{\partial I(i)} = \frac{R(i)}{|G(i)|^2} \quad (19)$$

$$\sigma_{\varphi(i)}^2 = (c_R \sigma_R)^2 + (c_I \sigma_I)^2 = \sigma_{\text{DFT}}^2 \frac{I^2 + R^2}{|G(i)|^4} = \frac{\sigma_{\text{DFT}}^2}{|G(i)|^2} \quad (20)$$

It is evident that the standard uncertainty of the phase depends on the amplitude of the component. Moreover, in the non-coherent sampling it changes with displacement δ as we will see in the following examples.

Frequency is known ($\sigma_\delta = 0$):

For intelligibility, one can omit index m in (10) $\varphi_a = \varphi(i) - a \cdot \delta + \pi/2$ and from (20) we get (Fig. 5a):

$$\frac{\sigma_{\varphi_a}}{\sigma_{\text{DFT}}} = \frac{1}{|G(i)|} \quad (21)$$

For the second estimation by $\varphi_b = (1 - s\delta)\varphi(i) + s\delta\varphi(i+s) + \pi/2$ (15) one needs sensitivity coefficients associated with the real and imaginary coefficients for two spectral lines $i, i+s$:

$$c_{R_b, i} = \frac{\partial \varphi_b(i)}{\partial R(i)} = (1 - s\delta)c_{R, i}; \quad c_{I_b, i} = \frac{\partial \varphi_b(i)}{\partial I(i)} = (1 - s\delta)c_{I, i}$$

$$c_{R_b, i+s} = \frac{\partial \varphi_b(i+s)}{\partial R(i+s)} = s\delta c_{R, i+s}; \quad c_{I_b, i+s} = \frac{\partial \varphi_b(i+s)}{\partial I(i+s)} = s\delta c_{I, i+s} \quad (22)$$

Since the correlation coefficients for the rectangular window $r(R(i), R(i+s))$ and $r(I(i), I(i+s))$ are zero and standard uncertainties are equal $\sigma_{R,*} = \sigma_{I,*} = \sigma_{\text{DFT}}$ ($* = i, i+s$) we can write according to [8] (Fig. 5b):

$$\left(\frac{\sigma_{\varphi_b}}{\sigma_{\text{DFT}}} \right)^2 = c_{R_b, i}^2 + c_{I_b, i}^2 + c_{R_b, i+s}^2 + c_{I_b, i+s}^2$$

$$\frac{\sigma_{\varphi_b}}{\sigma_{\text{DFT}}} = \sqrt{((1 - s\delta)/|G(i)|)^2 + (s\delta/|G(i+s)|)^2} \quad (23)$$

In calculations of the four sensitivity coefficients for the third estimation (24) one needs partial sensitivity coefficients for the amplitude $\partial|G(*)|/\partial R(*) = R(*)/|G(*)|$, $\partial|G(*)|/\partial I(*) = I(*)/|G(*)|$ and for the phase coefficients $\partial\varphi(*)/\partial R(*)$, $\partial\varphi(*)/\partial I(*)$ (19) since all of them contribute in the estimation:

$$\varphi_c = \frac{|G(i)|\varphi(i) + b|G(i+s)|\varphi(i+s)}{|G(i)| + b|G(i+s)|} + sa \left(\frac{b|G(i+s)|}{|G(i)| + b|G(i+s)|} - s\delta \right) + \frac{\pi}{2} \quad (24)$$

$$c_{R_c,*} = \frac{\partial \varphi_c(*)}{\partial R(*)}; \quad c_{I_c,*} = \frac{\partial \varphi_c(*)}{\partial I(*)} \quad (25)$$

In these case the uncertainty is close to the uncertainty of the estimation by (15) (Fig. 5c). Ratios of the uncertainties of the phase estimations related to the standard uncertainty of the amplitude DFT coefficient are between 2 and 3,5 symmetrically depending on the term δ at higher values of the relative frequency θ .

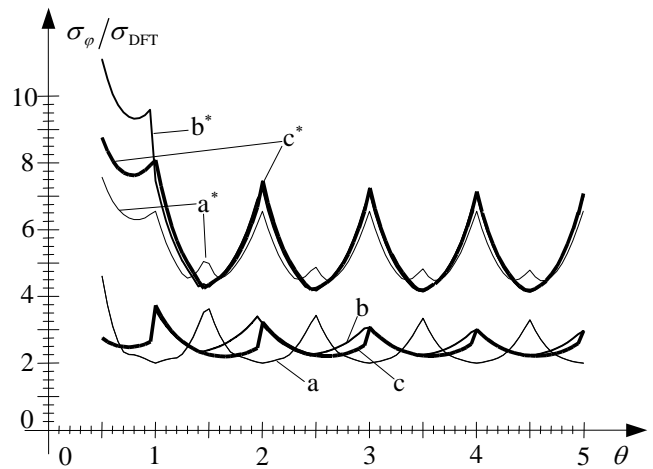


Fig. 5. Ratios of the uncertainties of the phase estimations related to the standard uncertainty of the amplitude DFT coefficient (dimensions in rd/V). Estimations: a – by (10), b – by (15), c – by

(17), θ is known; a^*, b^*, c^* - θ is estimated by (18)

Frequency is estimated by (18)

The uncertainties of the estimations increase if one needs to estimate also the displacement term $\delta(|G(i)|, |G(i+s)|)$. In the first estimation (10) one needs partial sensitivity coefficients also for the displacement term $\partial\delta/\partial|G(i)| = -s|G(i+s)|/(|G(i)|+|G(i+s)|)^2$ and $\partial\delta/\partial|G(i+s)| = s|G(i)|/(|G(i)|+|G(i+s)|)^2$.

$$\begin{aligned} c_{R_a,*} &= \frac{\partial\varphi_a}{\partial R(*)} = \frac{\partial\varphi(i)}{\partial R(*)} - a \cdot \frac{\partial\delta}{\partial|G(*)|} \cdot \frac{\partial|G(*)|}{\partial R(*)} \\ c_{I_a,*} &= \frac{\partial\varphi_a}{\partial I(*)} = \frac{\partial\varphi(i)}{\partial I(*)} - a \cdot \frac{\partial\delta}{\partial|G(*)|} \cdot \frac{\partial|G(*)|}{\partial I(*)} \end{aligned} \quad (26)$$

All the partial sensitivity coefficients except $\partial\varphi(i)/\partial R(i+s)$ and $\partial\varphi(i)/\partial I(i+s)$ are non-zero. The ratio of uncertainties is (Fig. 5 a*):

$$\begin{aligned} \left(\frac{\sigma_{\varphi_a}}{\sigma_{\text{DFT}}}\right)^2 &= c_{R_a,i}^2 + c_{I_a,i}^2 + c_{R_a,i+s}^2 + c_{I_a,i+s}^2 \\ \frac{\sigma_{\varphi_a}}{\sigma_{\text{DFT}}} &= \frac{1}{|G(i)|} \sqrt{1 + a^2 \left(\frac{|G(i)|}{|G(i)|+|G(i+s)|}\right)^2 - 2a^2 \frac{|G(i)|^3|G(i+s)|}{(|G(i)|+|G(i+s)|)^4}} \end{aligned} \quad (27)$$

In the second estimation (15) we have following dependencies $\delta(R(*), I(*))$, $\varphi(*) = \varphi(R(*), I(*))$ and the sensitivity coefficients are as follows:

$$\begin{aligned} c_{R_b,i} &= \frac{\partial\varphi_b}{\partial R(i)} = s(\varphi(i+s) - \varphi(i)) \cdot \frac{\partial\delta}{\partial R(i)} + (1-s\delta) \cdot \frac{\partial\varphi(i)}{\partial R(i)} \\ c_{I_b,i} &= \frac{\partial\varphi_b}{\partial I(i)} = s(\varphi(i+s) - \varphi(i)) \cdot \frac{\partial\delta}{\partial I(i)} + (1-s\delta) \cdot \frac{\partial\varphi(i)}{\partial I(i)} \\ c_{R_b,i+s} &= \frac{\partial\varphi_b}{\partial R(i+s)} = s(\varphi(i+s) - \varphi(i)) \cdot \frac{\partial\delta}{\partial R(i+s)} + s\delta \cdot \frac{\partial\varphi(i+s)}{\partial R(i+s)} \\ c_{I_b,i+s} &= \frac{\partial\varphi_b}{\partial I(i+s)} = s(\varphi(i+s) - \varphi(i)) \cdot \frac{\partial\delta}{\partial I(i+s)} + s\delta \cdot \frac{\partial\varphi(i+s)}{\partial I(i+s)} \end{aligned} \quad (28)$$

where we use $\partial\delta/\partial R(*) = \partial\delta/\partial|G(*)| \cdot \partial|G(*)|/\partial R(*)$ and $\partial\delta/\partial I(*) = \partial\delta/\partial|G(*)| \cdot \partial|G(*)|/\partial I(*)$. The ratio of uncertainties can be expressed as (Fig. 5 b*):

$$\begin{aligned} \left(\frac{\sigma_{\varphi_b}}{\sigma_{\text{DFT}}}\right)^2 &= (\varphi(i+s) - \varphi(i))^2 \frac{|G(i+s)|^2}{(|G(i)|+|G(i+s)|)^4} \left(\frac{R(i)}{|G(i)|}\right)^2 - \\ &- 2 \cdot (\varphi(i+s) - \varphi(i)) \cdot (1-s\delta) \cdot \frac{I(i)}{|G(i)|^2} \cdot \frac{|G(i+s)|}{(|G(i)|+|G(i+s)|)^2} \cdot \frac{R(i)}{|G(i)|} \end{aligned} \quad (29)$$

The uncertainty of the third estimation (Fig. 5 c*) is very close to the upper uncertainty (Fig. 5 b*) at higher values of the θ . Fig 5 shows that uncertainties of the estimations increase for a factor $2 \div 2,3$ if frequency is estimated by (18).

5. EXPERIMENTAL RESULTS

The methods were also tested by a real measurement system. In experiment we use sampling DVM (HP3458: $f_s = 25\text{kHz}$, $U_{\text{range}} = 10\text{V}$, $N = 1024$, time base accuracy: 0,01%, jitter $< 100\text{ps}$) and synthesizer/function generator (HP3325A: $f = 100\text{Hz}$, $u_{\text{pp}} = 20\text{V}$, frequency accuracy: $5 \cdot 10^{-6}$, triangle linearity: 0,05% of the range). Interpolation algorithms have been validated with the sine (Figs. 6 and 7) and triangular (Figs. 8, 9, and 10) shape signals.

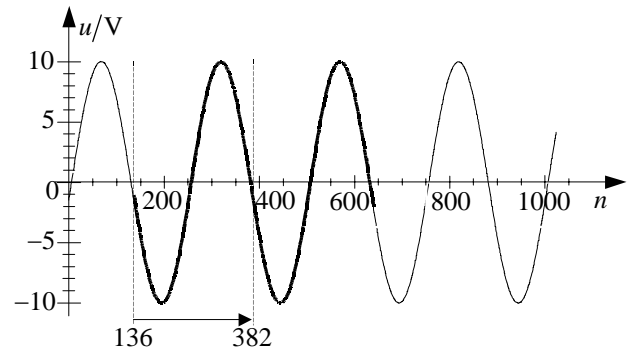


Fig. 6. Sampled sine function $N = 1024$ and truncated part $N_{\text{window}} = 505$ ($\theta = 2,02$)

The truncated window (the bold line in Fig. 6) has been moved for approximately one period (from point 136 to point 382). The estimations with interpolations algorithms (10), (15), (17), and (15) with the estimated displacement by (18) have been compared to the estimation by the coherent sampling window $N = 500 = 2 * f_s / f$ ($\theta = 2$) with the same first sampling point. The maximal errors of phase estimations $E_\varphi = \varphi(\theta = 2,02) - \varphi(\theta = 2)$ (Fig. 7) are close to the expected values in Fig. 4. The best results give us the estimation by (17) (Fig. 7c: $|E_\varphi|_{\text{max}} \approx 4 \cdot 10^{-5} \text{rd} \approx 2 \text{m}^\circ$).

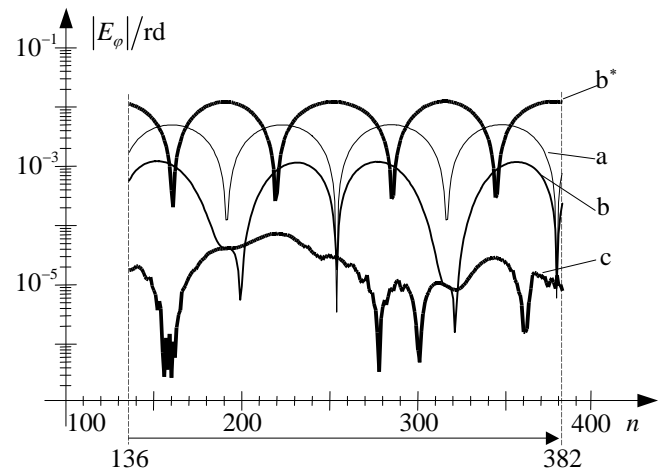


Fig. 7. The absolute values of errors of the phase estimations: a – by (10), b – by (15), c – by (17), b* – by (15) and θ is estimated by (18)

The triangular shaped signal (Fig. 8) has higher harmonics, which disturb the phase estimation of the fundamental component. At some values of the relative frequency the second estimation by (15) gives better results than by (17) since it doesn't emphasize only a single (fundamental) component (Fig. 9). The maximal values of errors are near $|E_\varphi|_{\max} \approx 10^{-3} \text{ rd} \approx 57 \text{ m}^\circ$.

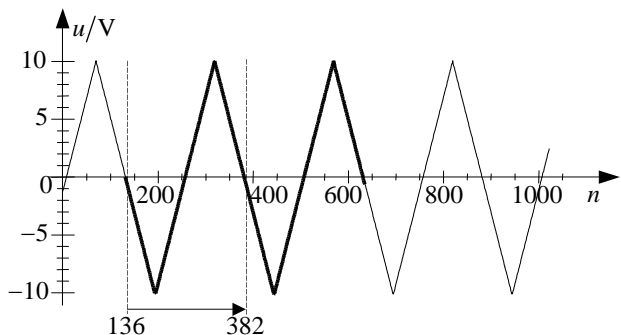


Fig. 8. Sampled triangular function $N = 1024$ and truncated part $N_{\text{window}} = 505$ ($\theta = 2,02$)

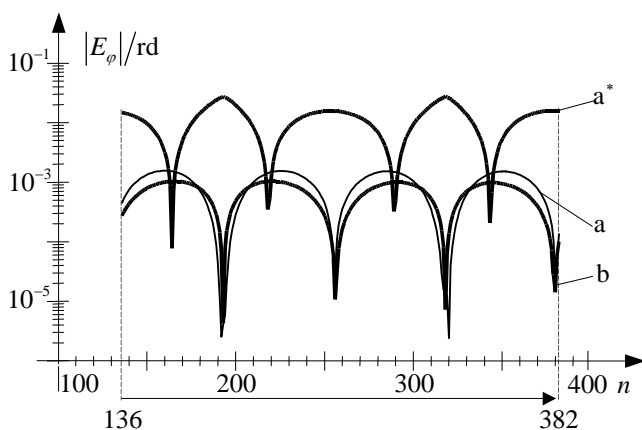


Fig. 9. The absolute values of errors of the phase estimations of the fundamental spectral component $\theta = 2,02$: a – by (15), b – by (17), a* – by (15) and θ is estimated by (18)

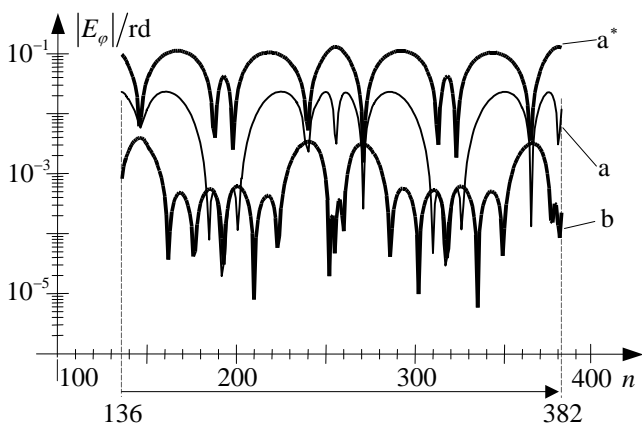


Fig. 10. . The absolute values of errors of the phase estimations of the third spectral component $\theta = 6,06$: a – by (15), b – by (17), a* – by (15) and θ is estimated by (18)

The amplitude of the third component is nine times smaller than the amplitude of the fundamental component and the uncertainty contribution to the estimation error relatively increases (Fig. 10).

4. CONCLUSIONS

In the paper, we have pointed out the advantages of the DFT interpolations for the phase estimation. Interpolations where the long-range leakage is considered decrease systematic effects. One possibility is an averaging of the two arguments surrounding the component (15). This estimation is independent of the number of the sampling points. Better estimation can be attained by considering also the long-range contributions (17). The error bound of the phase estimation is lower than $|E|_{\max} < 1 \text{ m}^\circ$, if we have enough periods of the signal in the measurement interval $\theta > 5$. When the measurement window is shortened to around two cycles of the signal errors increase to $|E|_{\max} < 2 \text{ m}^\circ$.

The simulation and experimental results show that the systematic errors and uncertainties almost symmetrically to the integer values of the relative frequency change with the displacement term δ in the non-coherent sampling.

REFERENCES

- [1] K.K. Clarke, D.T. Hess, "Phase Measurement, Traceability, and Verification Theory and Practice", *IEEE Trans. Instrum. Meas.*, vol. 39, no. 1, pp. 52-55, February 1990.
- [2] T. Grandke, "Interpolation Algorithms for Discrete Fourier Transforms of Weighted Signals", *IEEE Transactions on Instrumentation and Measurement*, vol. IM-32, no. 2, pp. 350-355, June 1983.
- [3] G. Andria, M. Savino, A. Trotta, "Windows and Interpolation Algorithms to Improve Electrical Measurement Accuracy", *IEEE Transactions on instrumentation and measurement*, vol. 38, no. 4, pp. 856-863, August 1989.
- [4] J. Schoukens, R. Pintelon, H. Van hamme, "The Interpolated Fast Fourier Transform: A Comparative Study", *IEEE Transactions on instrumentation and measurement*, vol. 41, no. 2, pp. 226-232, April 1992.
- [5] F. J. Harris, "On the Use of Windows for Harmonic Analysis with the Discrete Fourier Transform", *Proceedings of the IEEE*, vol. 66, no. 1, pp. 51-83, January 1978.
- [6] M. Bertocco, C. Offelli and D. Petri, "Dynamic Behavior of Digital Phase Estimator", *IEEE Trans. Instrum. Meas.*, vol. 41, no. 6, pp. 755-761, December 1992.
- [7] J. Scoukens, J. Renneboog, "Modelling the Noise Influence on the Fourier Coefficients After a Discrete Fourier Transform", *IEEE Transactions on instrumentation and measurement*, vol. IM-35, no. 3, pp. 278-286, September 1986.
- [8] International Org. for Standardization, *Guide to the Expression of Uncertainty in Measurements*, Geneva, Switzerland, 1995.

Author: Dr. Dušan Agrež, Faculty of Electrical Engineering, University of Ljubljana, Tržaška 25, 1000 Ljubljana, Slovenia, phone: +386 1 4768 220, fax: +386 1 4768 426 and e-mail: dusan.agrez@fe.uni-lj.si.